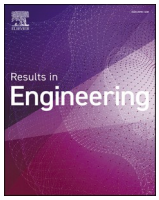
Results in Engineering 24 (2024) 102958



Contents lists available at ScienceDirect

Results in Engineering

journal homepage: www.sciencedirect.com/journal/results-in-engineering





Frequency regulation of PV-reheat thermal power system via a novel hybrid educational competition optimizer with pattern search and cascaded PDN-PI controller

Serdar Ekinci [a], Davut Izci [a,b,c], Ozay Can [d], Mohit Bajaj [e,f,g,*], Vojtech Blazek [h]

[a] Department of Computer Engineering, Batman University, Batman, 72100, Turkey
[b] Applied Science Research Center, Applied Science Private University, Amman, 11931, Jordan
[c] MEU Research Unit, Middle East University, Amman, 11831, Jordan
[d] Department of Electronics and Automation, Recep Tayyip Erdogan University, Rize, Turkey
[e] Department of Electrical Engineering, Graphic Era (Deemed to be University), Dehradun, 248002, India
[f] College of Engineering, University of Business and Technology, Jeddah, 21448, Saudi Arabia
[g] Graphic Era Hill University, Dehradun, 248002, India
[h] ENET Centre, VSB—Technical University of Ostrava, 708 00, Ostrava, Czech Republic

ARTICLE INFO

Keywords:
Educational competition optimizer
Pattern search
Cascaded PDN-PI controller
Two-area power system
Photovoltaic system
Load frequency control

ABSTRACT

Maintaining a stable balance between generated power and load demand is a critical challenge in modern power systems, especially with the increasing integration of renewable energy sources like photovoltaic (PV) systems. This study introduces a novel hybrid educational competition optimizer with pattern search (hECO-PS) algorithm to optimally tune a cascaded proportional-derivative with filter and proportional-integral (PDN-PI) controller for load frequency control (LFC) in a two-area power system comprising a PV system and a reheat thermal power system. The proposed hECO-PS algorithm enhances both global exploration and local exploitation capabilities, resulting in superior convergence rates and solution accuracy. The controller's performance was evaluated under various scenarios, including a 10 % step load change and solar radiation variations, demonstrating significant improvements in frequency regulation. The hECO-PS tuned PDN-PI controller achieved a minimum integral of time-weighted absolute error (ITAE) value of 0.4464, outperforming conventional methods like the modified whale optimization algorithm and sea horse algorithm, which yielded ITAE values of 2.6198 and 0.8598, respectively. Furthermore, the proposed controller reduced settling time by up to 46 % and minimized overshoot by up to 40 %. These results confirm the efficacy of the proposed approach in enhancing system stability and reliability under dynamic operating conditions, suggesting it as a promising solution for LFC in modern power systems with high renewable energy penetration.

1. Introduction

Ensuring adequate quality and reliable power for end-users is a fundamental principle of power systems. However, increases in load demands make it difficult to maintain the balance between production and consumption. Achieving the balance between production and consumption is possible through the establishment of active power balance. In the process of ensuring active power balance, it is planned to keep the grid frequency within certain levels. In other words, an imbalance in active power causes increases or decreases in system frequency. When the power demanded exceeds the power produced, the frequency decreases. Conversely, if the power demanded is less than the power produced, the frequency increases. Load frequency control (LFC) is a control process carried out to maintain balance by monitoring system frequency and changes in tie-line power.

The controller used in the LFC process is crucial for achieving successful results. In this process, classical controllers such as proportional-integral (PI) [1–4], proportional-integral-derivative (PID) [5,6], PID with filter (PIDN) [7,8] have been employed. However, these controllers are insufficient for solving complex problems. Therefore, fractional

* Corresponding author. Department of Electrical Engineering, Graphic Era (Deemed to be University), Dehradun, 248002, India.
E-mail addresses: serdar.ekinci@batman.edu.tr (S. Ekinci), davutizci@gmail.com (D. Izci), ozay.can@erdogan.edu.tr (O. Can), thebestbajaj@gmail.com (M. Bajaj), vojtech.blazek@vsb.cz (V. Blazek).

https://doi.org/10.1016/j.rineng.2024.102958
Received 15 August 2024; Received in revised form 14 September 2024; Accepted 20 September 2024
Available online 21 September 2024
2590-1230/© 2024 The Authors. Published by Elsevier B.V. This is an open access article under the CC BY-NC-ND license (http://creativecommons.org/licenses/by-nc-nd/4.0/).

order (FO) controllers [9] and cascade controllers [10] have been developed so far. Studies have shown that better results are achieved as the number of parameters to be optimized increases. Therefore, there is still room for improvement in the controller to be used.

Another alternative solution to LFC problem is the use of metaheuristic optimization techniques. The main advantage of these techniques is their ability to solve nonlinear functions. In this context, optimization techniques such as salp swarm algorithm (SSA) [11], black widow optimization algorithm (BWOA) [12], modified whale optimization algorithm (MWOA) [13], wild horse optimizer (WHO) [14], brown bear optimization algorithm (BOA) [15], sperm swarm optimization (SSO) [16] have been utilized by researchers in LFC process. However, according to the "No free lunch theorems for optimization," there is no guarantee that an algorithm will perform well for all problems [17]. Therefore, it is believed that newly developed optimization techniques may yield better results in the process [18]. For example, Irudayaraj et al. [19] explored a chaotic atom search optimization for LFC in interconnected systems with renewable sources, while Loka et al. [20] proposed a coordinated LFC approach using the DEMA-TD3 algorithm for smart hybrid power systems. Similarly, Fathy et al. [21] introduced a new fractional-order control method optimized using a skill optimization algorithm, and Khan et al. [22] employed a PIλ (1+PDF) controller with hybrid energy storage for systems with high renewable energy penetration. Other studies, such as Fadheel et al. [23, 24], have utilized hybrid optimization techniques like grey wolf-assisted sparrow search and sparrow search-optimized fractional virtual inertia control to improve frequency regulation. These recent contributions underline the importance of developing robust control strategies for renewable-dominated power systems and motivate the development of the novel hybrid optimization approach presented in this study.

Recent advancements in LFC of power systems have also focused on developing innovative controller structures to improve system stability, especially in the presence of renewable energy sources and energy storage devices [25]. Notable among these are the contributions by Çelik et al. [10,26,27], which explore various control strategies optimized by different algorithms. The study in Ref. [26] investigated the performance of a fuzzy 1PD-PI controller optimized using the salp swarm algorithm (SSA) for LFC in renewable energy-assisted thermal and hydro-thermal power systems. The study demonstrated that the SSA-optimized fuzzy controller effectively manages the dynamic responses of interconnected power systems with mixed energy sources, such as wind, solar, and hydro, by reducing frequency deviations and improving overall system stability. The study in Ref. [27] proposed a novel fuzzy 1PD-TI (proportional-derivative with integral action) controller for LFC in interconnected power systems, incorporating renewable power generation and energy storage devices. The study demonstrated that the fuzzy 1PD-TI controller, optimized using intelligent algorithms, could handle the nonlinearities and uncertainties of complex power systems, including the intermittency of renewable energy sources. The controller provided robust frequency regulation and minimized tie-line power deviations, indicating the effectiveness of fuzzy control in hybrid power systems with diverse energy storage technologies. Finally, the work in Ref. [10] introduced a new fractional order PI–fractional order PD cascade controller, designed using the dragonfly search algorithm, for advanced load frequency control of power systems. The fractional-order control strategy demonstrated superior performance in terms of damping oscillations, reducing overshoot, and minimizing settling time under various load disturbance scenarios. This approach underscores the potential of fractional-order controllers in improving the dynamic response and robustness of LFC systems, particularly in power systems with high penetration of renewable energy.

While these studies provide valuable insights into advanced control strategies for LFC, they also highlight the ongoing need for novel controller designs that can further enhance system stability, reliability, and robustness under varying operating conditions. For example, the amount of energy generated from photovoltaic (PV) systems varies [21] depending on environmental factors, which necessitates a more careful consideration in LFC process. In studies on LFC in power systems containing RES, it is observed that, except for a few studies, the variable nature of PV systems has not been taken into account. Ignoring this variability raises concerns about the efficiency of the LFC process. Considering this fact and the presented works, this study proposes a controller and an optimization technique for LFC process in a two-area power system consisting of one PV system and one reheat thermal system. In this context, a cascade controller, named PDN-PI, consisting of proportional-derivative with filter (PDN) and proportional-integral (PI) loops, and a hybrid algorithm named hybrid educational competition optimizer with pattern search (hECO-PS) are proposed for the first time. The presented PDN-PI cascade controller, optimized by the hECO-PS, offers several advantages over the previously proposed methods.

- Unlike traditional fuzzy logic and fractional-order controllers, the PDN-PI controller combines PDN and PI control loops, allowing for better control precision and adaptability.
- The integration of the hECO-PS algorithm optimizes the controller parameters more effectively, enhancing both global exploration and local exploitation capabilities. This hybrid approach ensures superior performance in terms of convergence speed, solution accuracy, and adaptability to dynamic changes in the system.
- The proposed method has demonstrated significant improvements in minimizing frequency deviations, reducing overshoot, and achieving faster settling times under various load scenarios. It also exhibits robustness under parameter uncertainty.

These advantages motivate the development and application of the PDN-PI controller with hECO-PS optimization for LFC in modern power systems, particularly those with high renewable energy penetration, where maintaining stability and reliability is increasingly challenging.

The performance of the proposed hECO-PS tuned PDN-PI controller is compared with methods such as modified whale optimization algorithm (MWOA), sea horse algorithm (SHO), gorilla troops optimization (GTO), and firefly algorithm (FA) for different scenarios.The contributions of the study to the literature can be summarized as follows.

- A cascade controller named PDN-PI has been proposed for LFC in a two-area PV-reheat thermal power system for the first time.
- A hybrid algorithm named hECO-PS has been developed to optimally tune the parameters of the proposed controller.
- The performance of the proposed hECO-PS tuned PDN-PI controller has been compared with the performance of controllers used in studies found in the literature.
- The effectiveness of the hECO-PS tuned PDN-PI controller in the LFC process has been demonstrated.

The rest of the paper is organized as follows: Section 2 provides an overview of the proposed hECO-PS algorithm, detailing its structure and

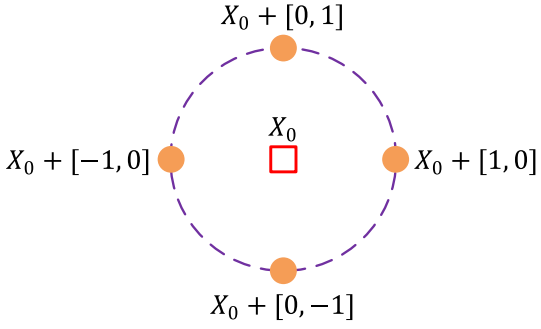


Fig. 1. Working mechanism of PS.

components. Section 3 introduces the power system model used for the LFC implementation. Section 4 presents the design and optimization process of the proposed PDN-PI controller. Section 5 discusses the simulation results, including comparisons with existing methods and analyses under varying operating conditions. Finally, Section 6 concludes the study and suggests potential future research directions.

2. Overview of ECO, PS and recommended hECO-PS

2.1. Educational competition optimizer (ECO)

The educational competition optimizer (ECO) is an algorithm developed to simulate the dynamics of educational competition by capturing competitive strategies observed at different educational levels such as primary school, middle school, and high school [28].

2.1.1. Phase 1: primary school phase

Throughout the primary school levels, schools determine appropriate teaching locations by considering the average location of the population. On the other hand, students set their individual goals by considering the proximity of neighboring schools. In each iteration, 20 % of the population categorized as schools based on suitability values, while the remaining 80 % continue as students. Primary school students prefer schools close to their homes due to factors such as safety and proximity. Additionally, educational institutions position themselves close to the students. In the pimary school phase of the ECO, the algorithm begins by determining teaching locations that are optimal for schools and students. The position of each school (X_i^{t+1}) in the next iteration ($t+1$) is calculated using Eq. (1):.

$$Schools: X_i^{t+1} = X_i^t + w \bullet \left(X_{imean}^t - X_i^t\right) \bullet Levy(dim) \quad (1)$$

where X_i^t is the current position of the school, w is an adaptive step size that decreases logarithmically with each iteration, X_{imean}^t is the average position of all schools, and $Levy(dim)$ represents a Levy flight distribution, which helps the algorithm explore the search space more effectively. Eq. (2) defines how students update their positions based on their proximity to schools:

Table 1
Parameter settings of hECO-PS and ECO algorithms for LFC problem.

Optimizer	Population size	Maximum iteration number	Other parameters
hECO-PS	50	100	$H = 0.5$, $initial_{mesh-size} = 1$, $mesh_{expansion-factor} = 2$, $mesh_{contraction-factor} = 0.5$ and $all_{tolerances} = 10^{-6}$
ECO	50	100	$H = 0.5$

$$Students: X_i^{t+1} = X_i^t + w \bullet \left(close\left(X_i^t\right) - X_i^t\right) \bullet randn \quad (2)$$

where $close\left(X_i^t\right)$ denotes the closest school to a student and $randn$ is a random number following a standard normal distribution. The weight factor w in Eq. (3) is adaptively adjusted to balance global exploration and local exploitation:

$$w = 0.1\ ln\left(2 - \frac{t}{Max_{iter}}\right) \quad (3)$$

which gradually decreases as the number of iterations (t) approaches the maximum iteration number (Max_{iter}).

2.1.2. Phase 2: middle school phase

During the middle school phase, schools use a more advanced method to choose teaching locations, taking into account both the best and average population locations. At the same time, students at this level establish their personal goals based on how close they are to neighboring schools. In each iteration, 10 % of the population is assigned as schools based on their suitability, while the remaining 90 % remain as students.

As academic pressure in middle school increases gradually, students are assigned a learning patience value denoted as P. They are divided into two groups based on whether they are academically rewarded or not. In this classification, the evaluation criterion H is set at 0.5. The learning motivation of academically rewarded students is represented by E, while this value is set to 1 for students who are not academically rewarded. w is referred to as the adaptive step size. During the middle school phase, a more refined search is performed. The patience value P

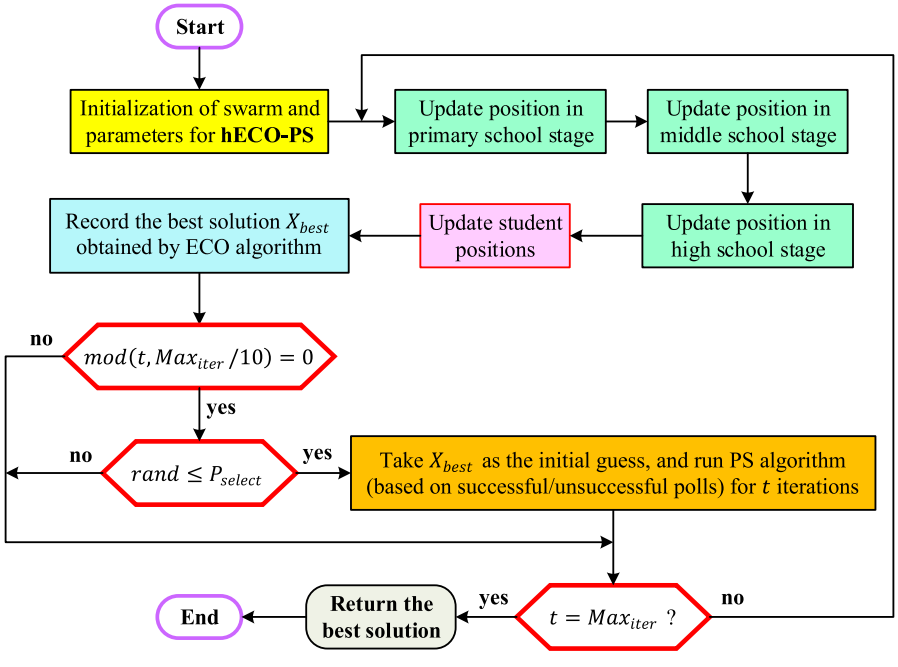


Fig. 2. Flowchart for hECO-PS.

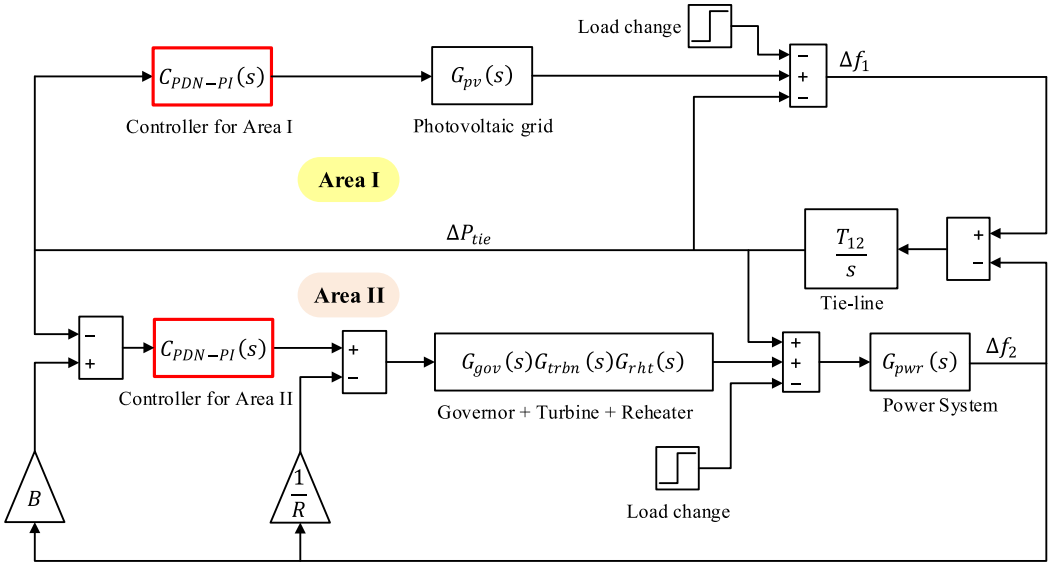


Fig. 3. Complete model of two-area power system with proposed controller.

in Eq. (4) helps divide students into groups based on their performance:

$$P = 4 \bullet randn \bullet \left(1 - \frac{i}{Max_{iter}}\right) \tag{4}$$

where i represents the current iteration. The motivation level E in Eq. (5) represents the learning effort of students:

$$E = \frac{\pi}{P} \bullet \frac{i}{Max_{iter}} \tag{5}$$

Eqs. (6) and (7) describe the update rules for schools and students, factoring in their proximity to both the best and mean population locations, and integrating Levy flight for effective exploration.

$$Schools: X_i^{t+1} = X_i^t + \left(X_{best}^t - X_{mean}^t\right) \bullet exp\left(\frac{i}{Max_{iter}} - 1\right) \bullet Levy(dim) \tag{6}$$

$$Students: X_i^{t+1} = \begin{cases} X_i^t - w \bullet close\left(X_i^t\right) - P \bullet \left(E \bullet w \bullet close\left(X_i^t\right) - X_i^t\right), R_1 < H \\ X_i^t - w \bullet close\left(X_i^t\right) - P \bullet \left(w \bullet close\left(X_i^t\right) - X_i^t\right), R_1 \geq H \end{cases} \tag{7}$$

The abilities of individual students are represented by a random number between 0 and 1, referred to as R_1.

2.1.3. Phase 3: high school phase

At the high school level, schools adopt a meticulous strategy for choosing teaching locations. They take into account not only the average population locations but also the best and worst locations within the populations. The optimization process motivates each student to aim for admission to the top high schools. During each iteration, 10 % of the population is assigned as specific schools according to their fitness values, while the remaining 90 % continue in their role as students. At the high school level, the algorithm emphasizes fine-tuning by considering both the best and worst locations. Eqs. (8) and (9) define how schools and students update their positions, integrating both random exploration (*randn*) and proximity-based adjustments:

$$Schools: X_i^{t+1} = X_i^t + \left(X_{best}^t - X_i^t\right) \bullet randn - \left(X_{best}^t - X_i^t\right) \bullet randn \tag{8}$$

$$Students: X_i^{t+1} = \begin{cases} X_{best}^t - P \bullet \left(E \bullet X_{best}^t - X_i^t\right), R_2 < H \\ X_{best}^t - P \bullet \left(X_{best}^t - X_i^t\right), R_2 \geq H \end{cases} \tag{9}$$

The abilities of individual students are represented by a random number between 0 and 1, referred to as R_2.

2.2. Pattern search algorithm (PS)

The Pattern Search (PS) technique [29] is employed to fine-tune solutions obtained from the ECO. PS is a derivative-free optimization method that alternates between directional search movements (DM) and pattern movements (PM). In DM, the algorithm searches along coordinate directions to detect potential improvements, while in PM, the algorithm explores nearby regions for local optimization, enhancing convergence speed and solution accuracy [30–36]. Considering the above explanation, Fig. 1 represents the working principle of the PS.

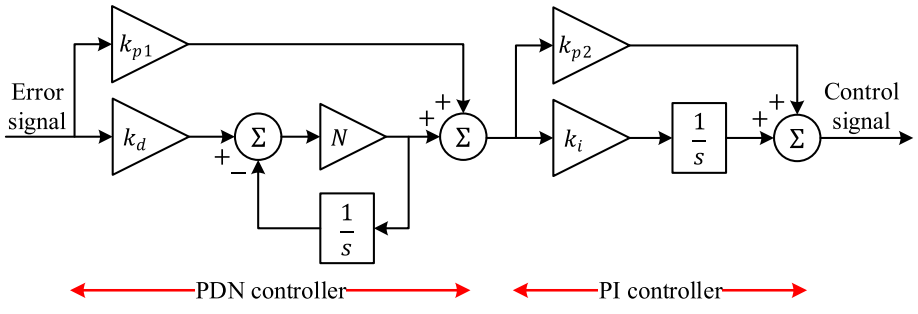


Fig. 4. Block diagram of cascaded PDN-PI controller.

2.3. Novel hybrid educational competition optimizer with pattern search (hECO-PS)

The hybrid educational competition optimizer with pattern search (hECO-PS) is an innovative approach combining the strengths of the ECO and the PS algorithm. The hECO-PS algorithm is designed to enhance the exploration and exploitation capabilities of the original ECO algorithm, leading to improved convergence rates and solution accuracy in complex optimization problems. The hybridization of ECO with PS integrates the exploratory capabilities of ECO with the local refinement strengths of PS. The strategy involves running the ECO algorithm to explore the global search space and identify promising regions. Once a promising region is identified, the PS algorithm is applied to fine-tune the solution by exploring the local neighborhood, ensuring that the solution is not only globally competitive but also locally optimized.

The framework of the hECO-PS algorithm is provided in Fig. 2. As seen, the initialization begins with an initial population of solutions, similar to ECO, where each solution represents a potential answer to the optimization problem. The ECO is applied to iteratively improve the population. During this phase, solutions undergo teaching, learning, and competition, allowing the population to converge towards promising areas of the search space. Then the PS is applied to the best solution (X_{best}) identified in the ECO phase to explore the local neighborhood, refining the solution by searching for improvements in a structured pattern. However, it is worth noting that the decision to implement the PS takes place after one tenth of the maximum iteration number. That means, the PS performs a total of 10 times during the process. In each call of the PS, a random number within 0, 1 is compared with a preselected (P_{Select}) number of 0.5. If the random number is higher than the preselected value, then the implementation of the PS is not performed. Otherwise, the PS takes the stage to improve the solution.

In order to ensure a clear understanding of the optimization processes employed in this study, the parameters for both the ECO and the hECO-PS have been summarized in Table 1. For the hECO-PS algorithm, parameters such as the population size, maximum iteration number, and specific settings for the PS technique, including the initial mesh size, mesh expansion factor, mesh contraction factor, and all tolerances, are provided. Similarly, for the ECO, key parameters such as population size, maximum iteration number, and the fitness evaluation threshold (H) are also listed. This detailed tabulation ensures transparency in our methodology and allows for accurate replication and validation of our results.

The hECO-PS algorithm, while offering improved exploration and exploitation capabilities over the standard ECO algorithm, presents certain limitations. It requires a slightly higher computational time due to the integration of the PS technique. Furthermore, the algorithm's performance is sensitive to key parameters, such as the number of iterations and population size. These parameters must be carefully selected and tuned based on the specific characteristics of the problem to ensure optimal performance.

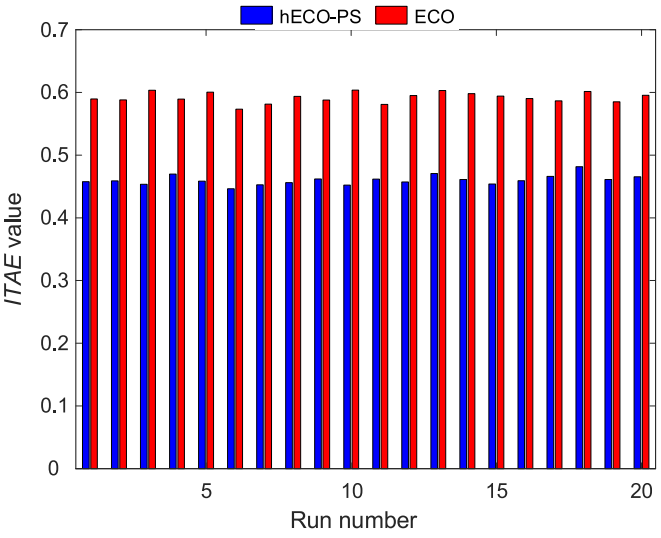


Fig. 6. Obtained ITAE values.

Table 2
Statistical performance metrics for ITAE.

Optimizer	Minimum	Maximum	Median	Average	SD
hECO-PS	0.4464	0.4814	0.4590	0.4603	0.0078
ECO	0.5733	0.6036	0.5918	0.5920	0.0084

3. Mathematical modeling of hybrid PV-thermal power system

In the study, the power system selected for load frequency control (LFC) consists of two areas: one is a PV system, and the other is a reheat thermal system. The PV system is designated as Area I, while the reheat thermal system is designated as Area II as shown in Fig. 3.

Area I. Photovoltaic system

The power value obtained from PV systems varies depending on factors such as irradiance and temperature. Therefore, circuits known as

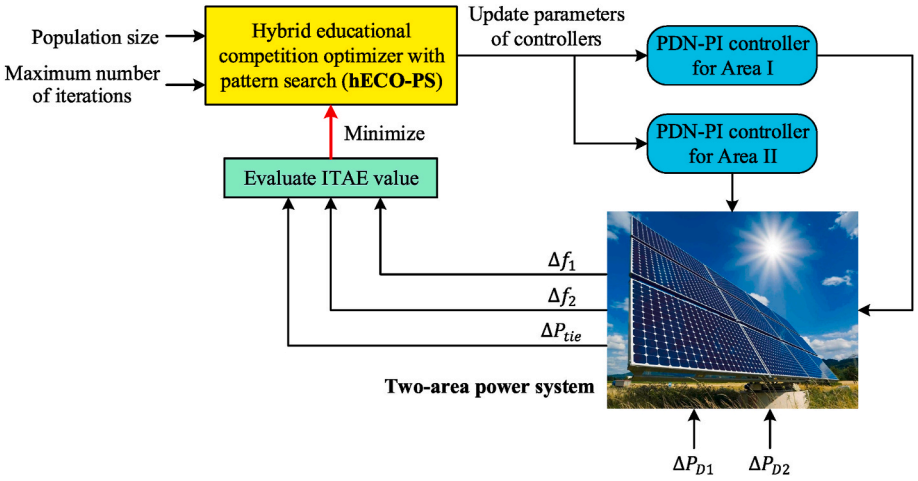


Fig. 5. HECO-PS based optimization process for load frequency control problem.

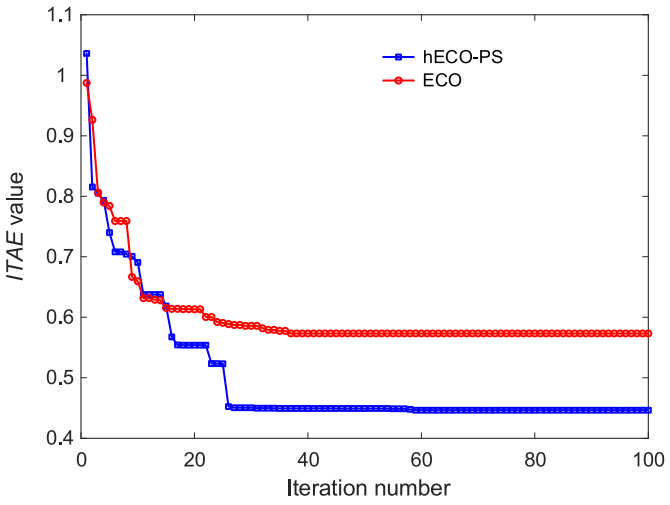


Fig. 7. Evolution of ITAE for hECO-PS and ECO.

Table 3
Limits of cascaded PDN-PI controller and optimized parameters.

Parameter		Lower limit	Upper limit	Optimized by hECO-PS	Optimized by ECO
Area I	k_{p1}	−2	2	−0.6953	−0.1532
	k_d	−2	2	−1.9345	−0.8146
	N	0.1	10	10	9.1685
	k_{p2}	0.01	2	1.6981	3.3813
	k_i	0.01	2	0.3648	1.8449
Area II	k_{p1}	−2	2	−2	−2
	k_d	−2	2	−0.6021	−1.4255
	N	0.1	10	10	10
	k_{p2}	0.01	2	1.5935	0.39578
	k_i	0.01	2	2	1.7131

maximum power point tracking (MPPT) are used to maximize this power value. Additionally, the energy obtained from PV systems is in DC form, and inverters are used to convert this form into AC. In line with all these, the transfer function for Area I, which includes components such as MPPT, inverter, and filter, is expressed by Eq. (10).

$$G_{pv}(s) = \frac{Ks + L}{s^2 + Ms + N} \tag{10}$$

In Eq. (10), $K = -18$, $L = 900$, $M = 100$ and $N = 50$.

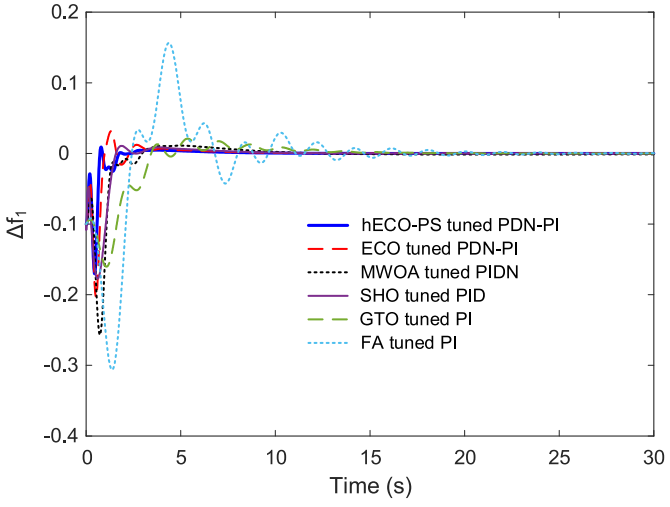


Fig. 8. Time response of Δf_1 for Case I.

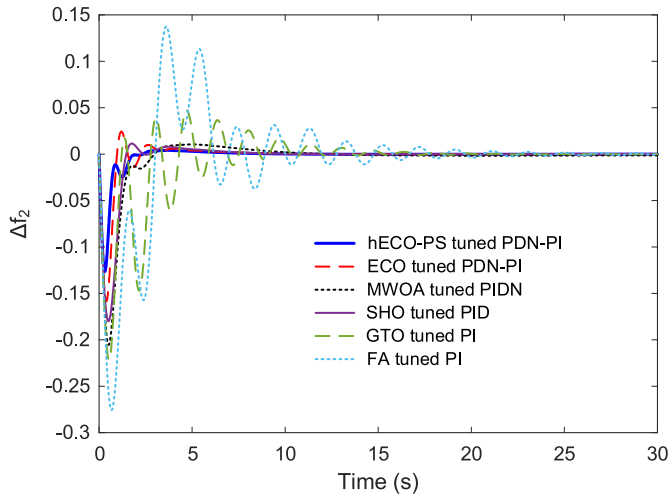


Fig. 9. Time response of Δf_2 for Case I.

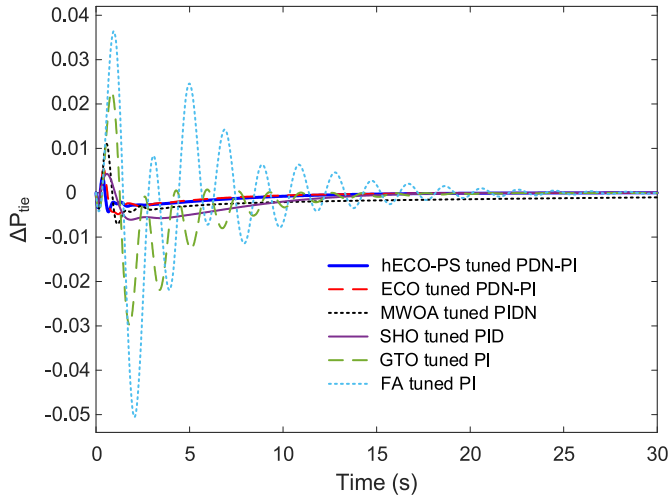


Fig. 10. Time response of ΔP_{tie} for Case I.

Table 4
Comparison of t_{set}, U_{min} and U_{max} for Case I.

Control method		t_{set} (s)	U_{min}	U_{max}
Δf_1	hECO-PS tuned PDN-PI	**0.5817**	−0.1704	**0.0091**
	ECO tuned PDN-PI	0.7316	−0.2041	0.0316
	MWOA tuned PIDN	1.0827	−0.2570	0.0111
	SHO tuned PID	1.0408	−0.1773	0.0108
	GTO tuned PI	1.6234	**−0.1603**	0.0209
	FA tuned PI	4.8609	−0.3063	0.1565
Δf_2	hECO-PS tuned PDN-PI	**0.4540**	**−0.1264**	**0.0041**
	ECO tuned PDN-PI	0.6525	−0.1585	0.0244
	MWOA tuned PIDN	0.9979	−0.2055	0.0105
	SHO tuned PID	0.9418	−0.1800	0.0115
	GTO tuned PI	2.4497	−0.2217	0.0471
	FA tuned PI	5.6082	−0.2757	0.1376
ΔP_{tie}	hECO-PS tuned PDN-PI	**0**	**−0.0043**	**0.0035**
	ECO tuned PDN-PI	**0**	−0.0048	0.0054
	MWOA tuned PIDN	**0**	−0.0071	0.0110
	SHO tuned PID	**0**	−0.0061	0.0043
	GTO tuned PI	1.9898	−0.0297	0.0227
	FA tuned PI	2.5018	−0.0505	0.0364

Area II. Reheat thermal system

The reheat thermal system consists of four different components: the governor, turbine, reheater, and power system. The transfer functions

and selected parameter values for these components are provided below. In these transfer functions, K_i represents the gain of the respective component, and T_i denotes the time constant of the respective component.

(a) Governor

$$G_{gov}(s) = \frac{K_G}{1 + sT_G} \tag{11}$$

In Eq. (11), $K_G = 1$ and $T_G = 0.08$ s.

(b) Turbine

$$G_{trbn}(s) = \frac{K_T}{1 + sT_T} \tag{12}$$

In Eq. (12), $K_T = 1$ and $T_T = 0.3$ s.

(c) Reheater

$$G_{rht}(s) = \frac{sK_R T_R}{1 + sT_R} \tag{13}$$

In Eq. (13), $K_R = 0.33$ and $T_R = 10$ s.

(d) Power system

$$G_{pwr}(s) = \frac{K_{PS}}{1 + sT_{PS}} \tag{14}$$

In Eq. (14), $K_{PS} = 120$ and $T_{PS} = 20$ s. In addition, $R = 2.5$ Hz/pu, $B = 0.8$ pu and $T_{12} = 0.545$.

4. Proposed controller and optimization process

4.1. Structure of cascaded PDN-PI controller

The proposed cascade PDN-PI controller in the study consists of two different loops. The first loop is a proportional-derivative (PD) with filter (PDN) controller, and the second loop is a proportional-integral (PI) controller. The transfer function of this cascade controller is represented by Eq. (15). In Eq. (15), k_{p1} represents the proportional gain in the first loop, k_d represents the derivative gain in the first loop, N is the filter coefficient, k_{p2} represents the proportional gain in the second loop, and k_i represents the integral gain in the second loop.

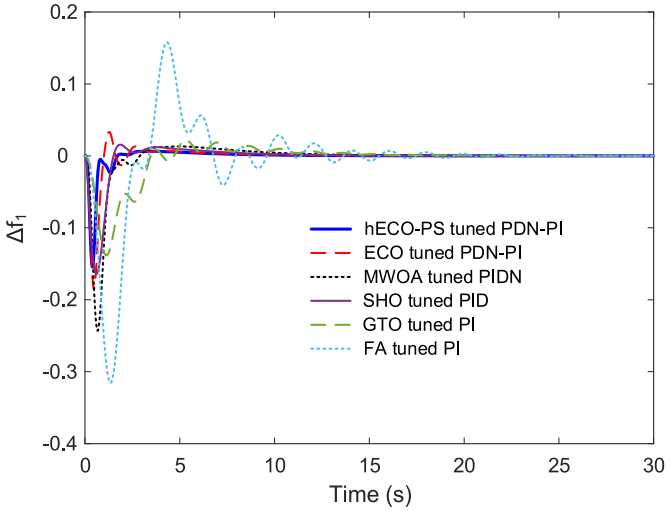


Fig. 11. Time response of Δf_1 for Case II.

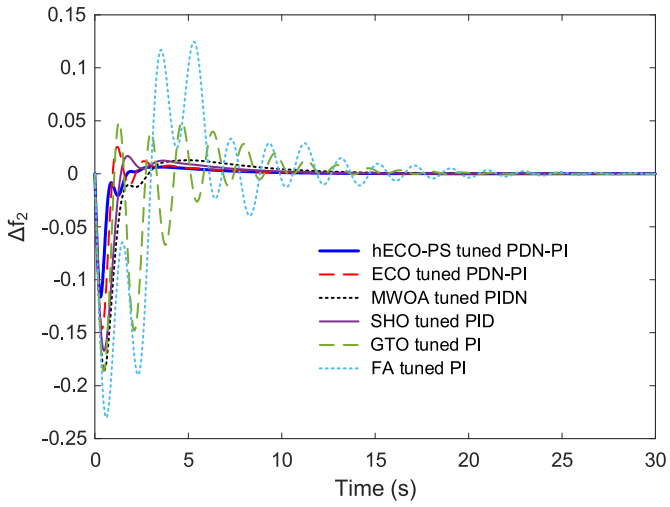


Fig. 12. Time response of Δf_2 for Case II.

$$C_{PDN-PI}(s) = \left(k_{p1} + k_d \frac{Ns}{s + N}\right) \times \left(k_{p2} + \frac{k_i}{s}\right) \tag{15}$$

The block diagram of the cascade controller is shown in Fig. 4.

4.2. Objective function

In this study, the integral of time-weighted absolute error (ITAE) objective function was selected to evaluate the performance of the proposed control method. The ITAE criterion is widely used in LFC studies because it emphasizes minimizing both the magnitude and duration of deviations from the desired frequency. This results in improved system stability and dynamic performance by penalizing prolonged errors more heavily. Furthermore, the ITAE objective function was chosen to maintain consistency with other recent studies in the literature where ITAE has been employed for performance evaluation. By adopting the same objective function, a fair and direct comparison of the effectiveness of different control strategies can be achieved. The transfer function of the ITAE objective function is given by Eq. (16). In the equation, t represents the time, Δf_1 denotes the frequency variation in Area I, Δf_2 denotes the frequency variation in Area II, and ΔP_{tie} represents the power change in the tie-line. During the optimization process, t_{sim} was set to 30 s.

$$ITAE = \int_0^{t_{sim}} t(|\Delta f_1| + |\Delta f_2| + |\Delta P_{tie}|)dt \tag{16}$$

The block diagram of LFC process for a two-area PV-reheat power system using hECO-PS tuned PDN-PI controller is shown in Fig. 5.

5. Simulation results

In this section of the study, several analyses have been conducted to evaluate the performance of the proposed hECO-PS technique. To achieve this, a comparison was first made between ECO and hECO-PS in terms of ITAE value. Subsequently, the performance of the proposed method was compared with the performance of methods from the literature, including MWOA tuned PIDN [1], SHO tuned PID [2], GTO tuned PI [3], and FA tuned PI [4], under different load variation conditions. In the next analysis, a comparison of ITAE values among these methods was performed. Finally, the system behavior was examined under solar radiation variation.

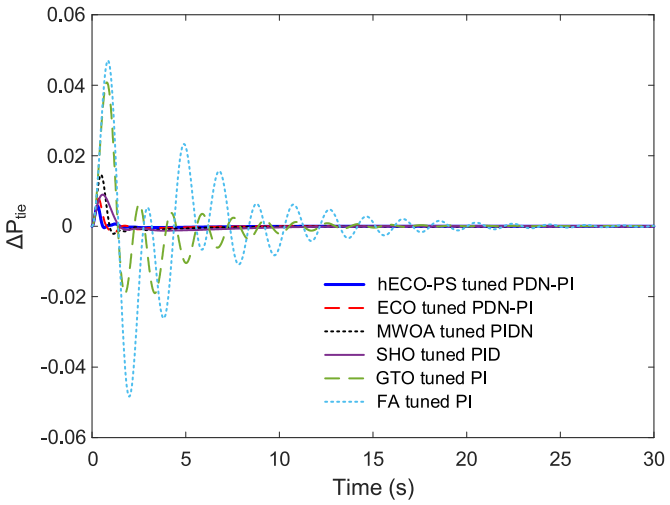


Fig. 13. Time response of ΔP_{tie} for Case II.

5.1. Application of hECO-PS and ECO algorithms

After performing 20 independent runs with a population size of 50 and 100 iterations, the ITAE values obtained for hECO-PS and ECO are shown in Fig. 6. The figure indicates that the designed hECO-PS tuned PDN-PI controller achieved a lower ITAE value compared to the ECO tuned PDN-PI controller for each run. The comparison results for the minimum, maximum, median, average, and standard deviation (SD) values obtained from the numerical data in Fig. 6 for hECO-PS and ECO are provided in Table 2. The data in the table show that the proposed method achieved lower values for all metrics. Additionally, the convergence curves for both algorithms over 100 iterations are presented in Fig. 7. In the optimization process, it is necessary to determine the lower and upper bounds for the parameters to be optimized [37]. Table 3 lists the specified lower/upper limits for each parameter and the optimal values obtained with both algorithms.

In addition to evaluating the performance of the proposed control strategies, the computation times for the optimization process were recorded to assess the computational efficiency of each algorithm. The average elapsed time per run was 1515.4 s for the ECO algorithm and 1642.4 s for the hECO-PS algorithm. The slightly higher computation time for the hECO-PS algorithm is attributed to the integration of the Pattern Search (PS) technique, which enhances the solution accuracy and robustness of the optimization process.

Table 5
Comparison of t_{set}, U_{min} and U_{max} for case II.

Control method		t_{set} (s)	U_{min}	U_{max}
Δf_1	hECO-PS tuned PDN-PI	**0.5327**	−0.1545	**0.0065**
	ECO tuned PDN-PI	0.7023	−0.1849	0.0333
	MWOA tuned PIDN	1.0504	−0.2431	0.0132
	SHO tuned PID	0.9891	−0.1642	0.0156
	GTO tuned PI	1.5515	**−0.1382**	0.0218
	FA tuned PI	4.8247	−0.3154	0.1579
Δf_2	hECO-PS tuned PDN-PI	**0.4193**	**−0.1163**	**0.0064**
	ECO tuned PDN-PI	0.6267	−0.1462	0.0254
	MWOA tuned PIDN	0.9780	−0.1856	0.0128
	SHO tuned PID	0.8910	−0.1671	0.0168
	GTO tuned PI	2.4046	−0.1863	0.0489
	FA tuned PI	5.6017	−0.2302	0.1246
ΔP_{tie}	hECO-PS tuned PDN-PI	**0**	**−4.2807E−04**	**0.0058**
	ECO tuned PDN-PI	**0**	−0.0020	0.0078
	MWOA tuned PIDN	**0**	−0.0022	0.0146
	SHO tuned PID	**0**	−0.0013	0.0090
	GTO tuned PI	1.1134	−0.0191	0.0408
	FA tuned PI	3.9307	−0.0483	0.0470

5.2. Comparisons with recently documented works

The performance of the proposed hECO-PS tuned PDN-PI method was evaluated under different conditions and compared with the performance of several studies reported in the literature.

Case I. 10 % step change in both areas ($\Delta P_{D1} = \Delta P_{D2} = 0.1$ p.u.)

In this case, the system behavior was analyzed for a 10 % load change, which corresponds to a 0.1 per-unit (p.u.) change, occurring in both areas of the system. The system responses Δf_1, Δf_2 and ΔP_{tie} obtained from the simulation studies using the optimal controller gains provided in Table 3 are shown in Figs. 8–10, respectively.

As seen in Figs. 8–10, under load change conditions in both areas, the proposed hECO-PS tuned PDN-PI controller resulted in smaller undershoot (U_{min}) and overshoot (U_{max}) values for Δf_1, Δf_2, ΔP_{tie} compared to the other methods. Additionally, when examining the settling time (t_{set}), which is the time required for the oscillations to damp, the proposed controller zeroed out the oscillations in a shorter period.

The numerical data obtained using Figs. 8–10 are presented in Table 4. Here, when calculating the settling times, a tolerance band of ±0.1 Hz was considered for Δf_1 and Δf_2, and a tolerance band of ±0.025 MW was used for ΔP_{tie}. As can be seen from the table, the proposed method provides a smaller U_{min}/ U_{max} and a shorter t_{set} compared to the other methods.

Case II. 10 % step change in Area II ($\Delta P_{D2} = 0.1$ p.u.)

In Case II, the system behavior was analyzed for a 10 % load change, which corresponds to a 0.1 p.u. change, occurring in Area II. The system responses Δf_1, Δf_2 and ΔP_{tie} obtained from the simulation studies using the optimal controller gains provided in Table 3 are shown in Figs. 11–13, respectively.

As seen in Figs. 11–13, under load change conditions in Area II, the proposed hECO-PS tuned PDN-PI controller resulted in smaller undershoot (U_{min}) and overshoot (U_{max}) values for Δf_1, Δf_2, ΔP_{tie} compared to the other methods. Additionally, when examining the settling time (t_{set}), which is the time required for the oscillations to damp, the proposed controller zeroed out the oscillations in a shorter period.

The numerical data obtained using Figs. 11–13 are presented in Table 5. Here, when calculating the settling times, a tolerance band of ±0.1 Hz was considered for Δf_1 and Δf_2, and a tolerance band of ±0.025 MW was used for ΔP_{tie}. As can be seen from the table, the proposed method provides a smaller U_{min}/ U_{max} and a shorter t_{set} compared to the other methods.

5.3. Comparison of ITAE performance metric

In an optimization problem, it is important for the selected objective function to converge to a certain value by the end of the specified number of iterations. Therefore, in this section, a comparison of ITAE values between the proposed method and the studies being compared has been carried out for Case I and Case II. The numerical data for this comparison can be seen in Table 6. As observed from the table, the proposed hECO-PS has provided the smallest ITAE values for both cases.

5.4. Influence of solar radiation variation

In this section, the effect of solar radiation variability on the performance of the proposed hECO-PS tuned PDN-PI controller is analyzed. Given that power generation from PV systems heavily depends on environmental conditions such as solar radiation and temperature, it is vital to evaluate the controller's robustness under these dynamic conditions to ensure stable LFC. To simulate realistic operating conditions, a maximum radiation change of to 0.2 pu was applied. Fig. 14 depicts the generated random power curve of the PV system in Area I under the

Table 6
ITAE values for various control methods.

Control method	Case I	Case II
hECO-PS tuned PDN-PI	**0.4464**	**0.4999**
ECO tuned PDN-PI	0.5733	0.6250
MWOA tuned PIDN	2.6198	1.5040
SHO tuned PID	0.8598	1.0528
GTO tuned PI	2.9185	3.0921
FA tuned PI	7.3783	7.4259

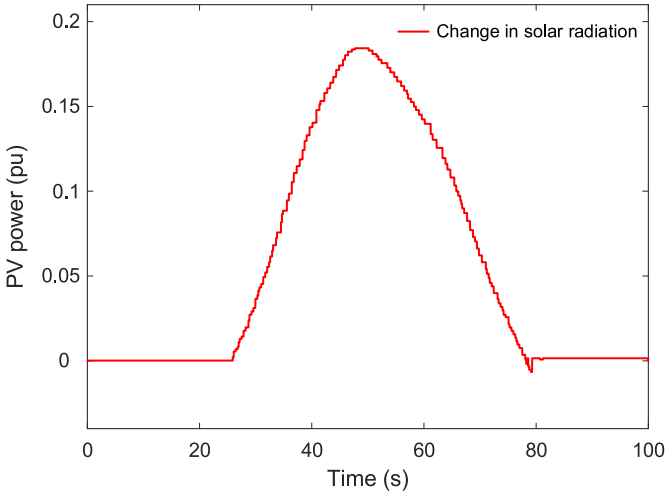


Fig. 14. Generated random power curve of PV in Area I.

applied solar radiation variations. The power output fluctuates to a maximum of up to 0.2 pu, representing typical variations due to changing solar radiation throughout the day. These fluctuation provide a realistic scenario for testing the adaptability and robustness of the proposed control method.

Fig. 15 presents the time response of the frequency deviations (Δf_1 and Δf_2) and tie-line power deviation (ΔP_{tie}) in the hybrid PV-thermal power system under solar radiation changes. The results indicate that the proposed hECO-PS tuned PDN-PI controller effectively maintains system stability despite the variations in solar radiation. The frequency deviations in both areas, (Δf_1 and Δf_2), show minimal overshoot and quickly return to their nominal values, demonstrating rapid stabilization. The tie-line power deviation, ΔP_{tie}, is kept within a narrow range, confirming the controller's ability to handle inter-area power exchanges effectively, even under fluctuating solar inputs.

5.5. Parameter variation test

To demonstrate the robustness and effectiveness of the proposed hECO-PS tuned PDN-PI controller under varying system parameters, a parameter variation test was conducted. This test considers the fault scenario described in Case I, with simultaneous ±25% variations in the time constants of key power system components, including the governor, turbine, reheater, and generator. These variations simulate real-world conditions where system parameters may fluctuate due to aging, maintenance, or environmental factors. Fig. 16 illustrates the time response of the frequency deviation in Area I (Δf_1) under parameter variations. As observed, the hECO-PS tuned PDN-PI controller effectively maintains system stability despite the ±25 % changes in parameter values. The response shows minimal overshoot and a rapid return to the nominal frequency, demonstrating the controller's robustness against significant parameter fluctuations.

Fig. 17 shows the time response of the frequency deviation in Area II (Δf_2) under the same parameter variations. Similar to the results in Area I, the proposed controller maintains a stable response with negligible overshoot and a quick settling time, even when the system's parameters are varied by ±25 %. This performance indicates the controller's ability to adapt to dynamic changes in the system configuration, ensuring reliable frequency regulation.

The time response of the tie-line power deviation (ΔP_{tie}) is presented in Fig. 18. The proposed hECO-PS tuned PDN-PI controller effectively manages the tie-line power flow, keeping deviations within a minimal range despite the significant parameter changes. The results highlight the controller's capacity to handle fluctuations in inter-area power exchange, which is crucial for maintaining overall system stability.

The results from Figs. 16–18 clearly demonstrate the effectiveness of the hECO-PS tuned PDN-PI controller in maintaining system stability and robustness under significant parameter variations. The controller's ability to handle such variations with minimal overshoot, fast settling time, and controlled tie-line power deviations suggests its high adaptability and reliability in real-world power system scenarios where parameter uncertainties are common.

5.6. Discussion on scalability and real-world applicability

The proposed hECO-PS algorithm has demonstrated its effectiveness in optimizing LFC for a two-area power system with renewable energy integration. However, its scalability to larger or more complex power systems and applicability in real-world scenarios require careful

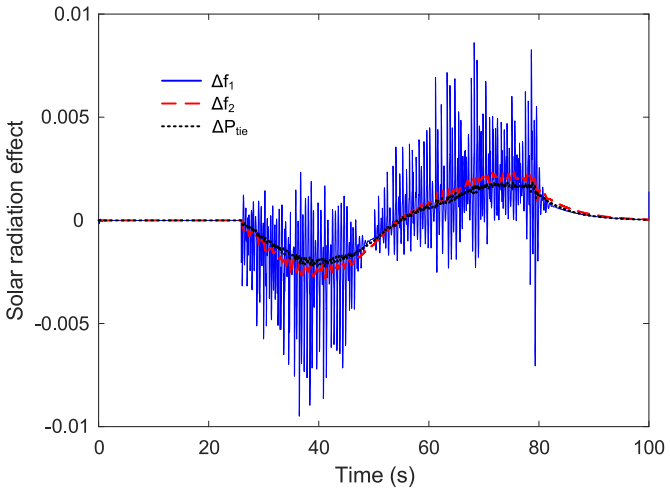


Fig. 15. Time response of hybrid PV-thermal power system.

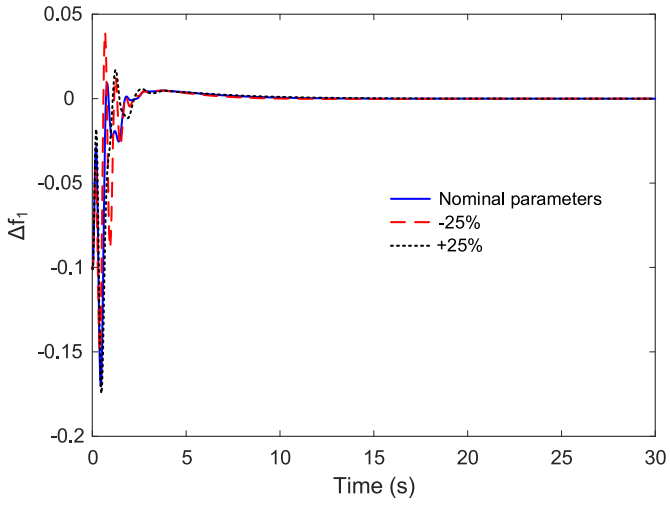


Fig. 16. Time response of Δf_1 under parameter variation.

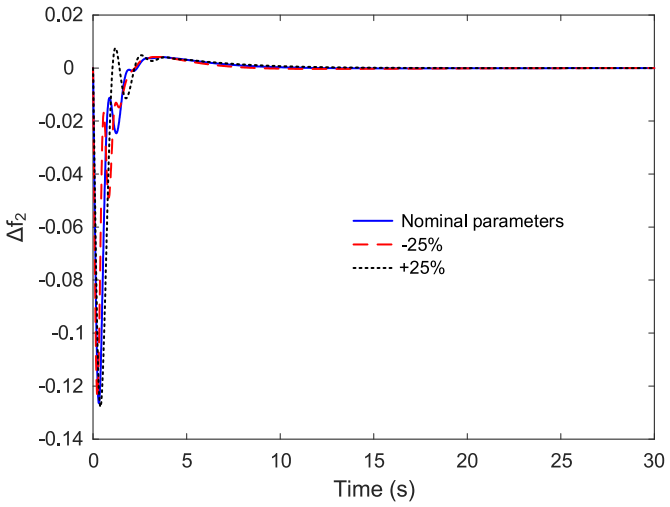


Fig. 17. Time response of Δf_2 under parameter variation.

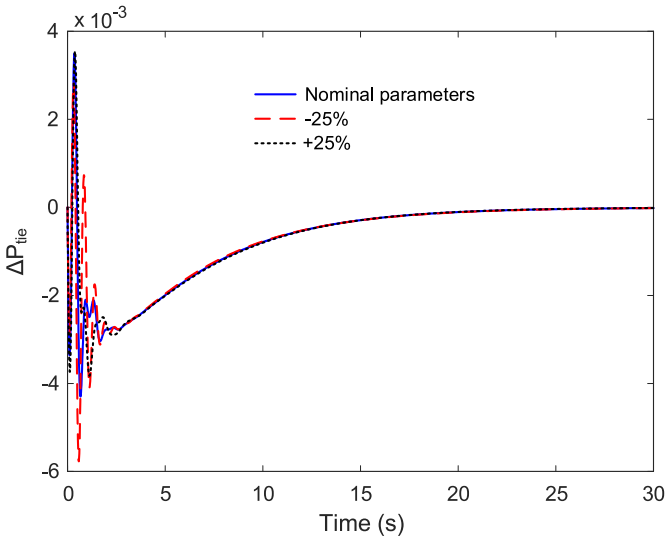


Fig. 18. Time response of ΔP_{tie} under parameter variation.

consideration. The hECO-PS algorithm is designed to efficiently handle a wide range of optimization problems due to its hybrid nature, combining the global search capabilities of the ECO with the local refinement provided by the PS technique. This hybrid approach allows the algorithm to scale effectively to larger power systems by maintaining an optimal balance between exploration and exploitation. The computational complexity remains manageable because the PS step is only triggered under specific conditions, reducing unnecessary computations. Therefore, the hECO-PS algorithm is expected to scale well with the increased number of generating units, transmission lines, and interconnected areas, typical in larger power systems.

For more complex power systems, such as those with multiple interconnected areas, high penetration of renewable energy sources, and varying load profiles, the adaptability of the proposed method becomes crucial. The algorithm's ability to dynamically adjust its parameters and fine-tune solutions based on current operating conditions makes it suitable for these environments. The integration of the PS technique allows for rapid convergence even in the presence of complex, nonlinear system dynamics, such as those seen in hybrid power systems with diverse energy sources (e.g., wind, solar, hydro, and storage systems).

In real-world scenarios, power systems are subject to various uncertainties, including fluctuations in renewable energy generation, load demand changes, and unexpected system disturbances. The proposed hECO-PS algorithm's flexibility and robustness make it particularly applicable under these varying conditions. Its hybrid nature enables it to quickly adapt to changing conditions by recalibrating its search strategy, ensuring reliable control performance across different scenarios. Additionally, the algorithm's low sensitivity to parameter settings and ability to handle multiple constraints simultaneously enhance its practical applicability in real-world environments.

The proposed method's applicability in real-world scenarios is further supported by its compatibility with existing power system infrastructure. Since the hECO-PS algorithm can be implemented in a decentralized or hierarchical control framework, it offers flexibility in integration with current control strategies and technologies used in modern power systems. Moreover, the algorithm's relatively low computational requirements, due to the selective use of the PS technique, make it suitable for real-time applications, where quick decision-making is crucial.

6. Conclusion and future research directions

In power systems, LFC is important for providing high-quality and reliable power. The increasing demand for loads makes this issue more complex, and thus it is frequently studied by researchers. To enhance the performance of the LFC process, it is necessary to use new types of controllers and newly developed optimization techniques. In this context, the current study presents a novel hybrid optimization algorithm, hECO-PS, integrated with a cascaded PDN-PI controller to enhance load frequency control in a two-area power system with renewable energy integration. The results demonstrate the effectiveness of the proposed controller in maintaining system stability under various dynamic conditions, including step load changes and solar radiation fluctuations. The hECO-PS algorithm showed superior performance compared to existing methods, achieving lower ITAE values, reduced settling times, and minimized overshoot. These improvements are attributed to the algorithm's ability to balance global exploration and local exploitation while optimizing the controller parameters. The proposed method is robust against parameter uncertainties and adaptable to real-world scenarios with varying conditions.

While the proposed hECO-PS tuned PDN-PI controller has shown promising results, several avenues for future research could further enhance its applicability and performance. Future research could extend the proposed method to more complex multi-area power systems, including a greater variety of renewable energy sources (RESs) such as wind and hydroelectric power. This would help validate the scalability and adaptability of the hECO-PS algorithm in more diverse and larger-scale environments. Investigating the integration of energy storage systems into the LFC framework could further improve system stability and performance, particularly in power systems with high penetration of RESs. Future work could focus on the real-time implementation of the proposed controller in actual power system environments. This would involve developing hardware-in-the-loop simulations or pilot projects in collaboration with industry partners to assess the practical viability and effectiveness of the method.

CRediT authorship contribution statement

Serdar Ekinci: Writing – original draft, Validation, Software, Methodology, Investigation, Formal analysis, Conceptualization. **Davut Izci:** Writing – review & editing, Writing – original draft, Supervision, Software, Project administration, Methodology, Investigation, Data curation, Conceptualization. **Ozay Can:** Supervision, Resources, Methodology, Formal analysis, Conceptualization. **Mohit Bajaj:** Writing – review & editing, Visualization, Supervision, Project administration. **Vojtech Blazek:** Writing – review & editing, Validation, Supervision, Project administration, Funding acquisition.

Declaration of competing interest

The authors declare that they have no known competing financial interests or personal relationships that could have appeared to influence the work reported in this paper.

Data availability

Data will be made available on request.

Acknowledgments

This article has been produced with the financial support of the European Union under the REFRESH – Research Excellence for Region Sustainability and High-tech Industries project number CZ.10.03.01/00/22_003/0000048 via the Operational Programme Just Transition and paper was supported by the following project TN02000025 National Centre for Energy II.

References

[1] R.K. Khadanga, A. Kumar, S. Panda, A novel modified whale optimization algorithm for load frequency controller design of a two-area power system composing of PV grid and thermal generator, Neural Comput. Appl. 32 (2020) 8205–8216, https://doi.org/10.1007/s00521-019-04321-7.
[2] C. Andic, S. Ozumcan, M. Varan, A. Ozturk, A novel sea horse optimizer based load frequency controller for two-area power system with PV and thermal units, International Journal of Robotics and Control Systems 4 (2024) 606–627, https://doi.org/10.31763/ijrcs.v4i2.1341.
[3] O. Can, M.S. Ayas, Gorilla troops optimization-based load frequency control in PV-thermal power system, Neural Comput. Appl. 36 (2024) 4179–4193, https://doi.org/10.1007/s00521-023-09273-7.
[4] S.M. Abd-Elazim, E.S. Ali, Load frequency controller design of a two-area system composing of PV grid and thermal generator via firefly algorithm, Neural Comput. Appl. 30 (2018) 607–616, https://doi.org/10.1007/s00521-016-2668-y.
[5] E. Çelik, Improved stochastic fractal search algorithm and modified cost function for automatic generation control of interconnected electric power systems, Eng. Appl. Artif. Intell. 88 (2020), https://doi.org/10.1016/j.engappai.2019.103407.
[6] S.P. Singh, T. Prakash, V.P. Singh, M.G. Babu, Analytic hierarchy process based automatic generation control of multi-area interconnected power system using Jaya algorithm, Eng. Appl. Artif. Intell. 60 (2017) 35–44, https://doi.org/10.1016/j.engappai.2017.01.008.
[7] S. Dewangan, T. Prakash, V. Pratap Singh, Design and performance analysis of elephant herding optimization based controller for load frequency control in thermal interconnected power system, Optim. Control Appl. Methods 42 (2021) 144–159, https://doi.org/10.1002/oca.2666.
[8] P.J. Krishna, V.P. Meena, N. Patnana, A. Mathur, V.P. Singh, Grey wolf optimizer-assisted R-method-based weighted minimization for automatic generation control in two-area interconnected power system, Int J Dyn Control 11 (2023) 1779–1796, https://doi.org/10.1007/s40435-022-01070-9.
[9] V. Padiachy, U. Mehta, Novel fractional-order proportional-integral controller for hybrid power system with solar grid and reheated thermal generator, Inside Solaris 3 (2023) 298–321, https://doi.org/10.3390/solar3020018.
[10] E. Çelik, Design of new fractional order PI–fractional order PD cascade controller through dragonfly search algorithm for advanced load frequency control of power systems, Soft Comput. 25 (2021) 1193–1217, https://doi.org/10.1007/s00500-020-05215-w.
[11] E. Çelik, N. Öztürk, E.H. Houssein, Influence of energy storage device on load frequency control of an interconnected dual-area thermal and solar photovoltaic power system, Neural Comput. Appl. 34 (2022) 20083–20099, https://doi.org/10.1007/s00521-022-07558-x.
[12] P. Dahiya, A.K. Saha, Frequency regulation of interconnected power system using black widow optimization, IEEE Access 10 (2022) 25219–25236, https://doi.org/10.1109/ACCESS.2022.3155201.
[13] R.K. Khadanga, A. Kumar, S. Panda, A novel modified whale optimization algorithm for load frequency controller design of a two-area power system composing of PV grid and thermal generator, Neural Comput. Appl. 32 (2020) 8205–8216, https://doi.org/10.1007/s00521-019-04321-7.
[14] A. Tabak, S. Duman, Maiden application of TIDμ1NDμ2 controller for effective load frequency control of non-linear two-area power system, IET Renew. Power Gener. 18 (2024) 1269–1291, https://doi.org/10.1049/rpg2.12817.
[15] S.K. Ojha, C.O. Maddela, Load frequency control of a two-area power system with renewable energy sources using brown bear optimization technique, Electr. Eng. 106 (2024) 3589–3613, https://doi.org/10.1007/s00202-023-02143-4.
[16] A. Deepa, A. Vinayagam, S.T. Suganthi, T. Kumaran, V. Veerasamy, R. Mohandas, A.X.R. Irudayaraj, An optimized frequency control of green energy integrated microgrid power system using modified SSO Algorithm, Soft Comput. 28 (2024) 6423–6446, https://doi.org/10.1007/s00500-023-09504-y.
[17] D.H. Wolpert, W.G. Macready, No Free Lunch Theorems for Optimization, 1997.
[18] K. Shejul, R. Harikrishnan, Energy consumption optimization of chiller plants with the genetic algorithm based GWO and JAYA algorithm in the dynamic pricing demand response, Results in Engineering 22 (2024) 102193, https://doi.org/10.1016/j.rineng.2024.102193.
[19] A.X.R. Irudayaraj, N.I.A. Wahab, M. Premkumar, M.A.M. Radzi, N. Bin Sulaiman, V. Veerasamy, R.A. Farade, M.Z. Islam, Renewable sources-based automatic load frequency control of interconnected systems using chaotic atom search optimization, Appl. Soft Comput. 119 (2022) 108574, https://doi.org/10.1016/j.asoc.2022.108574.
[20] R. Loka, R. Dubey, A.M. Parimi, Coordinated load frequency control of a smart hybrid power system using the DEMA-TD3 algorithm, Control Eng. Pract. 134 (2023) 105480, https://doi.org/10.1016/j.conengprac.2023.105480.
[21] A. Fathy, H. Rezk, S. Ferahtia, R.M. Ghoniem, R. Alkanhel, M.M. Ghoniem, A new fractional-order load frequency control for multi-renewable energy interconnected plants using skill optimization algorithm, Sustainability 14 (2022) 14999, https://doi.org/10.3390/su142214999.
[22] I.A. Khan, H. Mokhlis, N.N. Mansor, H.A. Illias, A. Daraz, A.K. Ramasamy, M. Marsadek, A.R. Afzal, Load frequency control in power systems with high renewable energy penetration: a strategy employing PIλ(1+PDF) controller, hybrid energy storage, and IPFC-FACTS, Alex. Eng. J. 106 (2024) 337–366, https://doi.org/10.1016/j.aej.2024.06.087.
[23] B.A. Fadheel, N.I.A. Wahab, A.J. Mahdi, M. Premkumar, M.A.B.M. Radzi, A.B. C. Soh, V. Veerasamy, A.X.R. Irudayaraj, A hybrid grey wolf assisted-sparrow search algorithm for frequency control of RE integrated system, Energies 16 (2023) 1177, https://doi.org/10.3390/en16031177.
[24] B.A. Fadheel, N.I.A. Wahab, P. Manoharan, A.J. Mahdi, M.A.B.M. Radzi, A.B. C. Soh, H.M. Ridha, A.R. Alsoud, V. Veerasamy, A.X.R. Irudayaraj, B.D. Alemu, A hybrid sparrow search optimized fractional virtual inertia control for frequency regulation of multi-microgrid system, IEEE Access 12 (2024) 45879–45903, https://doi.org/10.1109/ACCESS.2024.3376468.
[25] S. Priyadarshani, K.R. Subhashini, J.K. Satapathy, Design of an I + Fuzzy based PD control strategy for damping power system oscillations in a networked environment integrated with renewable energy sources, in: Advanced Frequency Regulation Strategies in Renewable-Dominated Power Systems, Elsevier, 2024, pp. 93–121, https://doi.org/10.1016/B978-0-323-95054-1.00017-2.
[26] E. Çelik, Performance analysis of SSA optimized fuzzy 1PD-PI controller on AGC of renewable energy assisted thermal and hydro-thermal power systems, J. Ambient Intell. Hum. Comput. 13 (2022) 4103–4122, https://doi.org/10.1007/s12652-022-03751-x.
[27] E. Çelik, N. Öztürk, Novel fuzzy 1PD-TI controller for AGC of interconnected electric power systems with renewable power generation and energy storage devices, Engineering Science and Technology, Int. J. 35 (2022) 101166, https://doi.org/10.1016/j.jestch.2022.101166.
[28] J. Lian, T. Zhu, L. Ma, X. Wu, A.A. Heidari, Y. Chen, H. Chen, G. Hui, The educational competition optimizer, Int. J. Syst. Sci. (2024), https://doi.org/10.1080/00207721.2024.2367079.
[29] S. Ghadami, H. Biglarian, H. Beyrami, M. Salimi, Optimization of multilateral well trajectories using pattern search and genetic algorithms, Results in Engineering 16 (2022) 100722, https://doi.org/10.1016/j.rineng.2022.100722.
[30] R.M. Rizk-Allah, A.E. Hassanien, A hybrid equilibrium algorithm and pattern search technique for wind farm layout optimization problem, ISA Trans. 132 (2023) 402–418, https://doi.org/10.1016/j.isatra.2022.06.014.
[31] V. Torczon, S.J. Optim, ON the convergence of pattern search algorithms. http://www.siam.org/journals/siopt/7-1/25078.html, 1997.
[32] D. Izci, S. Ekinci, An improved RUN optimizer based real PID plus second-order derivative controller design as a novel method to enhance transient response and robustness of an automatic voltage regulator, E-Prime - advances in Electrical Engineering, Electronics and Energy 2 (2022), https://doi.org/10.1016/j.prime.2022.100071.
[33] M. Eslami, E. Akbari, S.T. Seyed Sadr, B.F. Ibrahim, A novel hybrid algorithm based on rat swarm optimization and pattern search for parameter extraction of solar photovoltaic models, Energy Sci. Eng. 10 (2022) 2689–2713, https://doi.org/10.1002/ese3.1160.
[34] F. Wahid, R. Ghazali, Hybrid of firefly algorithm and pattern search for solving optimization problems, Evol Intell 12 (2019) 1–10, https://doi.org/10.1007/s12065-018-0165-1.
[35] D. Izci, S. Ekinci, M. Altalhi, M.S. Daoud, H. Migdady, L. Abualigah, A new modified version of mountain gazelle optimization for parameter extraction of photovoltaic models, Electr. Eng. (2024), https://doi.org/10.1007/s00202-024-02375-y.
[36] S. Ekinci, D. İzci, Pattern search ameliorated arithmetic optimization algorithm for engineering optimization and infinite impulse response system identification, ELECTRICA 24 (2024) 119–130, https://doi.org/10.5152/electrica.2023.22234.
[37] E. Çelik, N. Öztürk, A hybrid symbiotic organisms search and simulated annealing technique applied to efficient design of PID controller for automatic voltage regulator, Soft Comput. 22 (2018) 8011–8024, https://doi.org/10.1007/s00500-018-3432-2.